



# Epigenome-wide association study on methamphetamine dependence

Shirai, Toshiyuki ; Okazaki, Satoshi ; Tanifuji, Takaki ; Otsuka, Ikuo ; Horai, Tadasu ; Mouri, Kentaro ; Takemura, Yukihiro ; Aso, Katsuro ; ...

**(Citation)**

Addiction Biology, 29(3):e13383

**(Issue Date)**

2024-03

**(Resource Type)**

journal article

**(Version)**

Version of Record

**(Rights)**

© 2024 The Authors. Addiction Biology published by John Wiley & Sons Ltd on behalf of Society for the Study of Addiction.

This is an open access article under the terms of the Creative Commons Attribution-NonCommercial-NoDerivs License, which permits use and distribution in any medium, ...

**(URL)**

<https://hdl.handle.net/20.500.14094/0100487695>




## ORIGINAL ARTICLE

Addiction Biology

SSA

WILEY

# Epigenome-wide association study on methamphetamine dependence

Toshiyuki Shirai<sup>1</sup> | Satoshi Okazaki<sup>1</sup>  | Takaki Tanifuji<sup>1</sup> | Ikuo Otsuka<sup>1</sup> | Tadasu Horai<sup>1</sup> | Kentaro Mouri<sup>1</sup> | Yukihiro Takemura<sup>2</sup> | Katsuro Aso<sup>2</sup> | Noriya Yamamoto<sup>2</sup> | Akitoyo Hishimoto<sup>1</sup>

<sup>1</sup>Department of Psychiatry, Kobe University Graduate School of Medicine, Kobe, Japan

<sup>2</sup>Department of Psychiatry, Fukko-kai Tarumi Hospital, Kobe, Japan

## Correspondence

Satoshi Okazaki, BS, MD, PhD, Department of Psychiatry, Kobe University Graduate School of Medicine, 7-5-1 Kusunoki-cho, Chuo-ku, Kobe 650-0017, Japan.

Email: [okazakis@med.kobe-u.ac.jp](mailto:okazakis@med.kobe-u.ac.jp)

## Funding information

Japan Society for the Promotion of Science, Grant/Award Numbers: JP18K15483, JP21K07520, JP17H04249, JP21H02852

## Abstract

Repeated abuse of methamphetamine (METH) can cause dependence, repeated relapse of psychotic symptoms, compulsive drug-seeking behaviour, and various neurological symptoms. These long-term biological changes may be associated with epigenetic mechanisms; however, the association between METH use and epigenetic mechanisms has been poorly investigated. Thus, we performed an epigenome-wide association study of METH dependence using genomic DNA extracted from the blood samples of 24 patients with METH dependence and 24 normal controls. All participants were of Japanese descent. We tested the association between METH dependence and DNA methylation using linear regression analysis. We found epigenome-wide significant associations at four CpG sites, one of which occurred in the *CNOT1* gene and another in the *PUM1* gene. We especially noted the *CNOT1* and *PUM1* genes as well as several other genes that indicated some degree of association with METH dependence. Among the relatively enriched Gene Ontology terms, we were interested in terms of mRNA metabolism, respirasome, and excitatory extracellular ligand-gated ion channel activity. Among the relatively enriched Kyoto Encyclopedia of Genes and Genome pathways, we noted pathways of several neurological diseases. Our results indicate that genetic changes akin to those in other psychiatric or neurodegenerative disorders may also occur via epigenetic mechanisms in patients with METH dependence.

## KEYWORDS

DNA methylation, EWAS, methamphetamine

## 1 | INTRODUCTION

Methamphetamine (METH) abuse is a worldwide problem. METH is a powerful psychostimulant that facilitates the release of central and

peripheral monoamine neurotransmitters.<sup>1</sup> It frequently causes not only abuse but also dependence: nearly 34 million individuals use METH or other amphetamine-type stimulants, making it the third most widely used illegal drug worldwide.<sup>2</sup> One reason for the high

This is an open access article under the terms of the [Creative Commons Attribution-NonCommercial-NoDerivs](https://creativecommons.org/licenses/by-nc-nd/4.0/) License, which permits use and distribution in any medium, provided the original work is properly cited, the use is non-commercial and no modifications or adaptations are made.

© 2024 The Authors. *Addiction Biology* published by John Wiley & Sons Ltd on behalf of Society for the Study of Addiction.

prevalence of METH abuse is thought to be due to its 12-h half-life, which provides a longer lasting euphoric effect compared with other psychoactive substances.<sup>3</sup>

A low dose of METH can induce euphoria, tachycardia, mydriasis, and weight loss. This also causes an increase in arousal, elevates mood, lowers social inhibition, and lowers sexual inhibition.<sup>4</sup> High doses or repeated abuse can cause excessive drug-taking, compulsive drug-seeking behaviours, drug-taking behaviours, adverse social consequences, adverse medical consequences, paranoid delusions, auditory hallucinations, hyperactivity, repeated relapses of the psychotic disease, and various neurological symptoms.<sup>5,6</sup> These signs partially overlap with those of other psychiatric or neurological disorders such as schizophrenia, autism spectrum disorder, obsessive-compulsive disorder, mood disorder, and Parkinson's disease.<sup>7–9</sup> For example, elevated dopamine release is a common cause of the psychotic symptoms of METH dependence and schizophrenia, including auditory hallucinations and delusions.<sup>10</sup> Given the characteristics of these manifestations, METH dependence is characterized as a biological disorder thought to be the result of consequent molecular, cellular, and bio-pathological neuroadaptations akin to those observed in other psychiatric or neurodegenerative disorders.<sup>11</sup> Transient excessive monoamine neurotransmission alone is not sufficient to account for the long-lasting transcriptional and behavioural alterations.<sup>12</sup> Neurotransmission is related to DNA methylation differences and acts on transcriptional programs that underlie structural and neurobiological alterations.<sup>13,14</sup>

DNA methylation is an epigenetic mechanism that has recently garnered considerable attention. DNA methylation occurs mainly at cytosine-phosphate-guanine (CpG) sites. It causes the conversion of cytosine to 5-methylcytosine by DNA methyltransferase.<sup>15</sup> Although in practice, this may be more complicated, in principle, DNA methylation suppresses gene expression by affecting the interaction of chromatin proteins and certain transcription factors with DNA, rendering it integral to biological function.<sup>16</sup> Changes in DNA methylation patterns can maintain durable structural chromatin adaptations, leading to long-term dysregulation of biological processes and various related diseases.<sup>17</sup>

Many epigenetic studies have been performed in the fields of psychiatric disorders.<sup>18,19</sup> Several studies have also examined changes in human DNA methylation in METH use disorders.<sup>20,21</sup> For example, studies have reported a significant decline in DNA methylation associated with brain-derived neurotrophic factor (BDNF) in drug (METH and heroin) abusers than that in controls.<sup>22</sup> However, few studies have investigated the association between DNA methylation and METH use disorder or dependence, even though epigenetic modifications may potentially play key roles in drug-induced gene expression changes, given the long-term aspects of METH dependence.<sup>23</sup> Based on the symptom patterns of METH dependence, we postulated overlaps of associations similar to those seen in other psychiatric or neurological disorders such as schizophrenia, mood disorder, obsessive-compulsive disorder, and Parkinson's disease.

In the current study, we performed an epigenome-wide association study (EWAS) for more than 850,000 CpG sites to investigate the

association between DNA methylation patterns and METH dependence. We elucidated the epigenetic mechanisms in METH dependence and explored epigenetic factors that resulted in similar symptoms overlapped with those observed in other psychiatric or neurodegenerative diseases.

## 2 | METHODS

### 2.1 | Study sample

We obtained peripheral blood samples from 24 patients with METH dependence as the disease group. We also obtained samples from 24 age- and sex-matched control participants for comparison as the control group. All participants were of Japanese descent. This study was conducted in Kobe, Japan. Each patient was evaluated by at least two psychiatrists based on the criteria mentioned in the Diagnostic and Statistical Manual of Mental Disorders, Fourth Edition. The healthy controls were also assessed by at least two psychiatrists and screened for psychiatric disorders using unstructured interviews. The lack of a present, past, or family history (first-degree relatives) of psychiatric disorders or substance abuse (excluding nicotine dependence) was also confirmed in the control group. Written informed consent was obtained from all participants before study commencement, per the Declaration of Helsinki. This study was approved by the Ethical Committee for Genetic Studies of Kobe University Graduate School of Medicine.

### 2.2 | Data curation

DNA methylation analysis was performed as previously described.<sup>24</sup> We extracted genomic DNA from peripheral blood samples using the QIAamp DNA Blood Midi Kit (Qiagen, Hilden, Germany). Genomic DNA was bisulfite-converted, purified, and recovered using the EZ DNA Methylation Kit (ZYMO RESEARCH, Murphy Avenue, Irvine, CA, USA). A total of 250 ng of DNA was used for analysis. Bisulfite-converted DNA was amplified, fragmented, purified, and remixed in Buffer RA1 (Takara Bio, Shiga, Japan). The remixed DNA was hybridized with Infinium MethylationEPIC BeadChip (Illumina, San Diego, CA, USA), and screened using iScan (Illumina, San Diego, CA, USA).

From the fluorescence image data, the normalization was performed by Background Subtraction and Internal Controls, using GenomeStudio (ver. V2011.1)/Methylation Module (ver. 1.9.0). The degree of methylation was estimated via the fluorescence intensity ratio as any value between  $\beta = 0$  (unmethylated) to 1 (fully methylated), respectively. For normalization, each  $\beta$  value was corrected using the BMIQ method supplied with the R package, ChAMP. For each  $\beta$  value, the detection  $p$  value was computed from the background model characterizing the chance that the target sequence signal was distinguishable from the negative controls with GenomeStudio.

Probes with detection  $p$  values  $>0.01$  in one or more samples were designated as invalid and eliminated. Furthermore, we eliminated

probes located within five base pairs of single nucleotide polymorphisms (SNPs) with minor allele frequencies  $>0.05$ . Probes located on sex chromosomes were also eliminated. We also removed cross-reactive probes using the R package, maxprobes (ver. 0.0.2). We also designated probes having missing  $\beta$  values for all samples in either group as inappropriate. After filtering, 85 058 of 865 918 probes were judged invalid, and the remaining 780 860 probes were analysed. We got gene names relevant to each probe according to the complete GENCODE annotation in the Illumina manifest file. Also, cell type proportion was estimated using the Houseman method from the online DNA Methylation Age Calculator (<https://horvath.genetics.ucla.edu/html/dnamage/>, last accessed on 6 February 2023), using the Houseman et al. dataset background. Horvath calculator uses Houseman method.<sup>25,26</sup>

### 2.3 | Investigation of the association between DNA methylation and METH dependence

We tested the association between METH dependence and DNA methylation in 780 860 valid probes via linear regression analysis for phenotypes (disease group or control group), using the R package, limma (ver. 3.52.4), in conjunction with the empirical Bayes method. The  $\beta$  values were converted to  $M$  values for analysis [ $M = \log_2(\beta/(1 - \beta))$ ]. We used sex, age, and smoking history as covariates for the first regression model. We used sex, age, smoking history, and each cell type proportion as covariates for the second regression model. Due to the small sample size of this study, we decided to use the results of the first regression model for further analyses, considering the number of appropriate confounding factors, but we further examined the validity of the results by checking the Pearson's correlation of regression coefficients for phenotypes in both models. The  $p$  values were corrected using the Benjamini Hochberg (BH) method to calculate the  $q$  values. We defined probes that met  $q$  values  $<0.05$  as significant. Moreover, we selected the corresponding positions of the probes meeting the unadjusted  $p$  value  $<1.0 \times 10^{-5}$  criterion as the differentially methylated positions (DMPs).

Further, we conducted a weighted gene co-methylation network analysis (WGCNA), using the R package, WGCNA. We selected the probes having variance of  $M$  values up to the top 50 000 among all. To construct modules, the soft-thresholding power was set to 8 to maximize a scale-free topology model fit as it plateaued above 0.8. The module assignments were determined by using the blockwiseModules function with TOMType = "unsigned", minClusterSize = 100, reassignThreshold = 0, and mergeCutHeight = 0.25. For each participant, we calculated the value of module eigengene of each module. We conducted Pearson's correlation analysis for each variable (disease group or control group, age, sex, and smoking history) and each module eigengene. We calculated correlation coefficients and Student asymptotic  $p$  values for given correlations. The  $p$  values were adjusted with BH method considering multiple testing to calculate  $q$  values. We defined  $q < 0.05$  as significant.

Furthermore, using the R package, DMRcate (ver. 2.14.1), we identified the differentially methylated regions (DMRs) from CpG sites meeting the false discovery rate (FDR)  $< 0.08$ , according to the  $q$  value of the probe having unadjusted  $p$  value closest to  $1.0 \times 10^{-5}$ . We set  $\lambda = 1000$  and  $C = 2$ . Bases more than  $\lambda$  apart cannot be in the same region. The Gaussian kernel function is defined by  $k(x_1, x_2) = \exp(-\sigma[x_1 - x_2]^2)$ , calculated as  $\lambda/C = \sigma$ . DMRcate calculates kernel estimates using a Gaussian kernel function to identify DMRs.<sup>27</sup>

### 2.4 | Enrichment analysis

We performed Gene Ontology (GO) and Kyoto Encyclopedia of Genes and Genomes (KEGG) pathway analyses for genes relevant to DMPs. The BiomaRt R package (ver. 2.52.0) was used to convert gene names to Entrez gene IDs for the analysis. GO analysis was conducted with the R package, clusterProfiler (ver. 4.4.4). Background genes were acquired from geneList included in the R package, DOSE (ver. 3.22.1). KEGG pathway analysis was conducted online on the DAVID site (<https://david.ncifcrf.gov/>, last accessed on 9 April 2023). We noted GO terms and KEGG pathways meeting the criterion for unadjusted  $p < 0.01$ .

### 2.5 | Statistical analysis

Statistical analysis was conducted using R version 4.2.1 and EZR version 1.55. Age, body mass index (BMI), and each cell type proportion were compared using the Mann-Whitney  $U$  test. Fisher's exact test was employed for comparing smoking history, and the  $\chi^2$  test was used for comparing sex differences between the METH and control groups. As mentioned, linear regression analysis was performed for each probe to investigate the association between METH dependence and DNA methylation. Dummy variables were used as needed. For the phenotype: controls = 0, patients = 1, for the sex: male = 0, female = 1, for smoking history: never = 0, ever = 1, current = 2. In the correlation analyses, we used Pearson's method. Statistical calculations in the GO analysis were performed using the clusterProfiler R package, and the KEGG pathway analysis was performed using DAVID.

## 3 | RESULTS

### 3.1 | Demographic data

The demographic data of the two groups are listed in Table 1, and cell type proportion data are displayed in Figure S1. There was no significant difference for each cell type. We did not have BMI data for four patients with METH dependence. The missing values were compensated with the average of the remaining 20 patients with METH dependence.

**TABLE 1** Demographic data for the disease group and control group, respectively.

	Disease	Control	<i>p</i> value
Sample	24	24	
Age (years), median (IQR)	40.5 (31, 50)	40 (29.5, 48.25)	0.869 <sup>a</sup>
Age of first drug abuse, median (IQR)	22 (18, 26)		
Total duration of drug abuse (months), median (IQR)	126 (57, 219)		
BMI (IQR)	24.182 (21.826, 25.753)	22.472 (20.316, 24.419)	0.056 <sup>a</sup>
Smoking history (never/ever/current)	2/0/22	15/4/5	<0.001 <sup>b</sup>
Sex (male/female)	19/5	19/5	1 <sup>c</sup>

Note: For smoking history, “never” refers to individuals who have never smoked a cigarette, “ever” refers to individuals who used to smoke cigarettes in the past but stopped during blood sampling, and “current” refers to individuals who retained the smoking habit during blood sampling.

Abbreviations: BMI, body mass index; IQR, interquartile range.

<sup>a</sup>We assessed the *p* value using the Mann–Whitney *U* test.

<sup>b</sup>We assessed the *p* value using Fisher's exact test.

<sup>c</sup>We assessed the *p* value the using  $\chi^2$  test.

### 3.2 | Investigation of the association between DNA methylation and METH dependence

We tested the association between METH dependence and DNA methylation by subjecting 780 860 probes to linear regression analyses. For the first model, four probes met the  $q < 0.05$  criterion upon correction of the *p* values using the BH method. The *CNOT1* (cg22331182,  $p = 9.02 \times 10^{-9}$ ,  $q = 7.04 \times 10^{-3}$ ) and *PUM1* (cg07335637,  $p = 4.06 \times 10^{-8}$ ,  $q = 1.59 \times 10^{-2}$ ) genes were included in these significant positions. A total of 96 probes met the unadjusted  $p < 1.0 \times 10^{-5}$  criterion (76 hypomethylated and 20 hypermethylated), and we defined these corresponding positions as DMPs. Though there was no significant difference, the ratio of promoter regions was 36.1% in DMPs, compared with 30.8% in non-DMPs (unadjusted  $p = 0.26$  by Fisher's exact test). Ratios were calculated also for each gene regulatory region and compared between DMPs and non-DMPs by Fisher's exact test, adjusting the *p* values by BH method to calculate *q* values. No region met  $q < 0.05$ . (Figure S2). The top 12 probes for hypomethylated positions and hypermethylated positions in the first model are listed in Table 2. All probes that met the unadjusted  $p < 1.0 \times 10^{-5}$  condition are listed in Table S1. These relevant genes included *PSMA6* (cg18492497,  $p = 3.80 \times 10^{-7}$ ), *NDUFS3* (cg15346359,  $p = 4.88 \times 10^{-7}$ ), *TTC19* (cg09595082,  $p = 9.27 \times 10^{-7}$ , cg17360273,  $p = 2.81 \times 10^{-6}$ ), *GRIK2* (cg10769416,  $p = 2.43 \times 10^{-6}$ ), *EIF4ENIF1* (cg01168649,  $p = 3.77 \times 10^{-6}$ ), *NDUFS6* (cg21638645,  $p = 4.25 \times 10^{-6}$ ), *CHRNA2* (cg07054263,  $p = 5.41 \times 10^{-6}$ ), *BDNF-AS1* (cg03552992,  $p = 5.76 \times 10^{-6}$ ), *P2RX5* (cg07991565,  $p = 5.76 \times 10^{-6}$ ), *MAPK8* (cg02480970,  $p = 6.14 \times 10^{-6}$ ), and *TUBA8* (cg16193078,  $p = 9.96 \times 10^{-6}$ ). The Manhattan plot for the *p* values of 780 860 probes is shown in Figure 1, and the volcano plot is displayed in Figure S3. For the second model, only one probe, associated with *CNOT1*, was found to be significant (cg22331182,  $p = 2.84 \times 10^{-8}$ ,  $q = 2.22 \times 10^{-2}$ ). The top 12 probes for hypomethylated positions and hypermethylated positions in the second model are listed in

Table S2. The regression coefficients for the phenotype of each probe in both models were significantly correlated (correlation coefficient = 0.92,  $p < 2.2 \times 10^{-16}$ ) (Figure S4). The subsequent downstream analysis was performed on the results of the first model.

### 3.3 | WGCNA

Using the *M* values of probes having variance in the top 50 000 among all, we performed WGCNA. A total of 50 modules were created from these 50 000 probes. The eigengene of each module in each participant was calculated, and we conducted Pearson's correlation analysis for each variable (disease group or control group, age, sex, and smoking history) and each module eigengene. The details of each module eigengene are listed in Table S3. After adjustment with the BH method, there were no modules meeting  $q < 0.05$  for the association with METH dependence, except MEgrey ( $q = 0.022$ ), which is the eigengene of a set of CpGs that do not belong to any module suggesting co-methylation. The correlation heatmap for each module and each variable is displayed in Figure S5.

### 3.4 | DMRs analysis

The CpG site having unadjusted *p* value closest to  $1.0 \times 10^{-5}$  had *q* value with  $8.00 \times 10^{-2}$ . Using R package DMRcate, we identified 13 DMRs from CpG sites meeting the FDR < 0.08. (Table S4). Four regions were hypomethylated and nine regions were hypermethylated. Hypomethylated regions included genes of *CNOT1*, *SNORA50*, *GRP133*, *RP11-76C10.2*, and *VARS*. Hypermethylated regions include genes of *ELK3*, *BHLHE40-AS1*, *EFNA4*, *EFNA3*, *ITFG2*, *NRIP2*, *NOL12*, *TRIOBP*, *CCNG1*, *RP11-541P9.3*, *DHX38*, *TXNL4B*, *AKAP8L*, and *KLLN*. The circos plot showing the relative positioning of DMRs on the chromosomes is displayed in Figure 2.

**TABLE 2** Hypomethylated/hypermethylated positions with top 12 *p* values in the linear regression model with age, sex, and smoking history as covariates (the first model).

Target ID	CHR	MAPINFO	GENE NAME	Beta dif	<i>p</i> value	<i>q</i> value
Hypomethylated positions						
cg22331182	16	58593647	CNOT1	−0.016999016	$9.02 \times 10^{-9}$	$7.04 \times 10^{-3}$
cg14785914	15	45725895	RP11-519G16.5	−0.015635916	$4.06 \times 10^{-8}$	$1.59 \times 10^{-2}$
cg07335637	1	31453133	PUM1	−0.066458256	$1.09 \times 10^{-7}$	$2.83 \times 10^{-2}$
cg22657302	2	123412924		−0.053388966	$1.78 \times 10^{-7}$	$3.48 \times 10^{-2}$
cg18492497	14	35746932	PSMA6, KIAA0391	−0.017696554	$3.80 \times 10^{-7}$	$5.11 \times 10^{-2}$
cg16219773	5	151812935	NMUR2	−0.074640462	$3.94 \times 10^{-7}$	$5.11 \times 10^{-2}$
cg15346359	11	47606064	NDUFS3	−0.01001938	$4.88 \times 10^{-7}$	$5.11 \times 10^{-2}$
cg06417215	16	3281522		−0.054594863	$5.52 \times 10^{-7}$	$5.11 \times 10^{-2}$
cg14575983	5	99922152	FAM174A	−0.051868782	$6.34 \times 10^{-7}$	$5.11 \times 10^{-2}$
cg09759578	19	1913405	SCAMP4, ADAT3	−0.023120599	$7.52 \times 10^{-7}$	$5.11 \times 10^{-2}$
cg23151747	3	18372447	TBC1D5	−0.018136141	$8.11 \times 10^{-7}$	$5.11 \times 10^{-2}$
cg16537749	17	59668583	AC002994.1, NACA2	−0.014797917	$8.94 \times 10^{-7}$	$5.11 \times 10^{-2}$
Hypermethylated positions						
cg07835814	20	32077669	CBFA2T2	0.008384167	$6.79 \times 10^{-7}$	$5.11 \times 10^{-2}$
cg05267543	1	155036802		0.00437187	$1.57 \times 10^{-6}$	$6.18 \times 10^{-2}$
cg18559739	6	4775132	RP3-430A16.1, CDYL	0.011602421	$1.81 \times 10^{-6}$	$6.18 \times 10^{-2}$
cg09665311	1	33429393		0.006894712	$1.82 \times 10^{-6}$	$6.18 \times 10^{-2}$
cg04302752	2	32264493	DPY30	0.002882227	$2.70 \times 10^{-6}$	$6.65 \times 10^{-2}$
cg21613631	7	82201725		0.003020239	$2.74 \times 10^{-6}$	$6.65 \times 10^{-2}$
cg01368133	4	89513561	HERC3	0.004923814	$3.06 \times 10^{-6}$	$6.65 \times 10^{-2}$
cg07147063	16	67260764	TMEM208, LRRC29	0.005689221	$3.58 \times 10^{-6}$	$6.65 \times 10^{-2}$
cg01168649	22	31892074	EIF4ENIF1, SFI1, DRG1	0.002111429	$3.77 \times 10^{-6}$	$6.65 \times 10^{-2}$
cg25158678	12	51785362	GALNT6, SLC4A8	0.004032259	$3.96 \times 10^{-6}$	$6.65 \times 10^{-2}$
cg21638645	5	1800072	MRPL36, NDUFS6	0.006066793	$4.25 \times 10^{-6}$	$6.65 \times 10^{-2}$
cg16338822	20	30326883	TPX2	0.001550931	$4.32 \times 10^{-6}$	$6.65 \times 10^{-2}$

Note: “CHR” represents the chromosome number and “MAPINFO” represents the chromosome coordinates. Gene names are written according to the complete GENCODE annotation. The term “beta dif” represents the difference between the means of the  $\beta$  values for each group (disease group – control group). The *p* values, which are unadjusted, indicate the degree of association between methamphetamine dependence and DNA methylation, calculated by linear regression analysis, and *q* values are the results of *p* values subjected to Benjamini Hochberg correction. The probes without relevant genes are blank for the GENE NAME column.

### 3.5 | Enrichment analysis

We performed GO and KEGG pathway analyses for the genes relevant to DMPs. GO analysis revealed 14 terms that met the unadjusted  $p < 0.01$  criterion (Table S5), including several terms relevant to mRNA metabolism (containing *CNOT1*, *PUM1*, and *EIF4ENIF1* genes), respirasome (containing *NDUFS3*, *NDUFS6*, and *TTC19* genes), and terms of excitatory extracellular ligand-gated ion channel activity (containing *CHRNA2*, *GRIK2*, and *P2RX5* genes). The R package clusterProfiler was used to create a barplot (Figure 3A), dot plot (Figure 3B), and cnetplot (Figure 4) for these terms. In the KEGG pathway analysis, five pathways met the unadjusted  $p < 0.01$  (Table S6), including several pathways relevant to neurological diseases (containing *TUBA8*, *PSMA6*, *MAPK8*, *NDUFS3*, and *NDUFS6* genes).

## 4 | DISCUSSION

We performed an EWAS to investigate the association between DNA methylation and METH dependence using peripheral blood samples. Although a few probes showed significant associations, we investigated *CNOT1*, *PUM1*, *NDUFS6*, *GRIK2*, and *BDNF-AS1*, which were parts of genes relevant to DMPs, by searching the relevant literature discussing the relationships with psychiatric or neurological disorders. We were also interested in the pertinent GO terms (mRNA metabolism, respirasome, and excitatory extracellular ligand-gated ion channel activity) and KEGG pathways (several neurological disorders) evinced throughout our analysis. In WGCNA, ME<sub>grey</sub> was significantly associated with METH dependence, but ME<sub>grey</sub> is the eigen-gene of a set of CpGs that do not belong to any of the modules that indicate co-methylation. We conducted literature research focusing



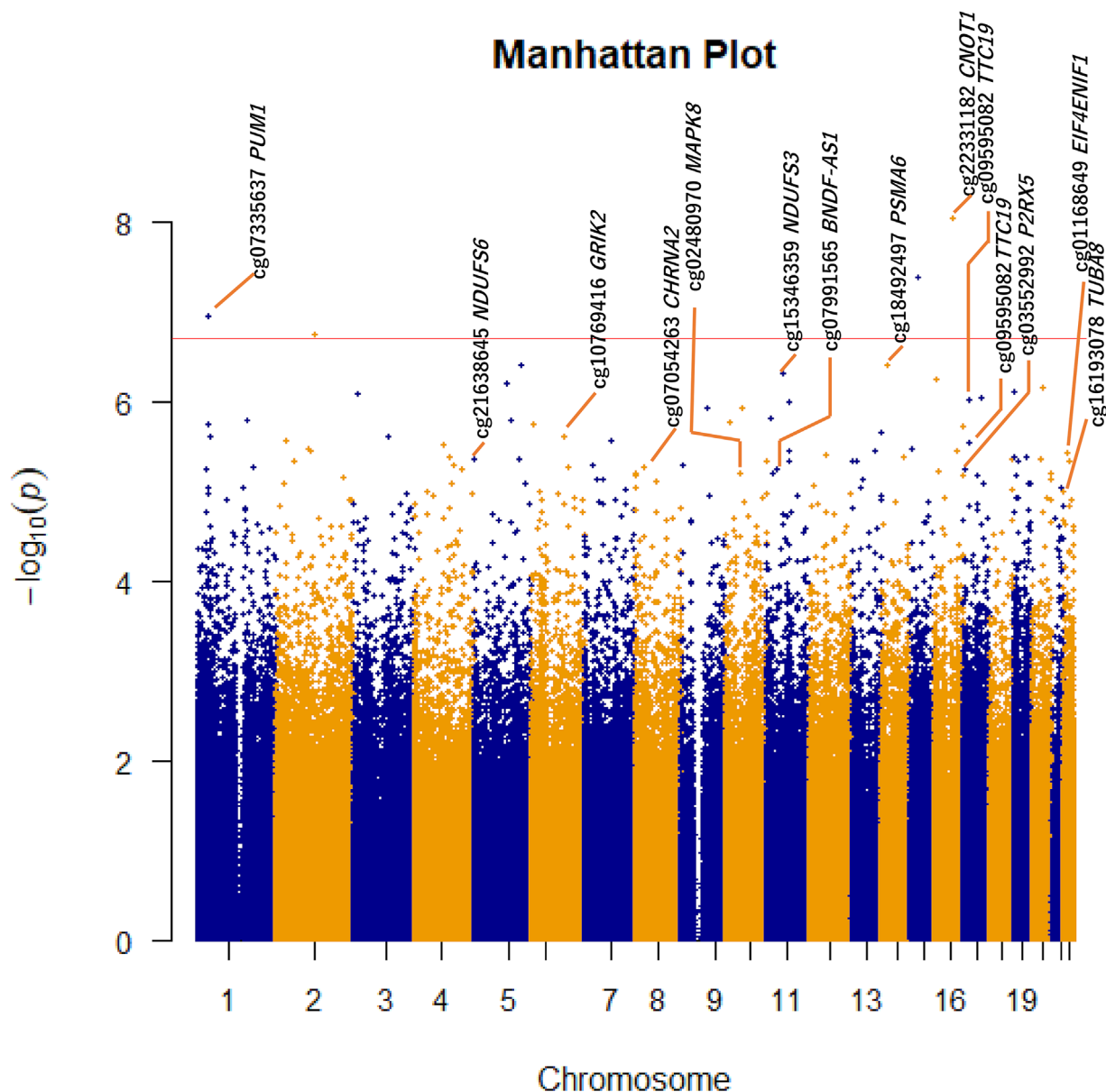


**FIGURE 1** Manhattan plot of  $p$  values calculated by linear regression analyses. The horizontal axis represents the corresponding chromosome and chromosome coordinates, and the vertical axis represents  $-\log_{10}(p)$ . This figure was created using the R package, manhattanly (ver. 0.3.0). The red line parallel to the horizontal axis indicates significance after Benjamini Hochberg adjustment. The plots of the probes of interest have been highlighted

on genes associated with probes having significant findings, genes for interesting GO terms and KEGG pathways, and genes closely related to those noted in previous METH studies.

#### 4.1 | CNOT1 and PUM1

The *CNOT1* gene was relevant to the probe with a significant change in DNA methylation in the disease group compared with the control group in the current study ( $q = 7.04 \times 10^{-3}$ ,  $p = 9.02 \times 10^{-9}$ ). This position was hypomethylated in the disease group. This position also indicated significant finding in the second model, and *CNOT1* was

also included in one DMR. This gene codes for CCR4-NOT transcription complex subunit 1 (*CNOT1*), involved in mRNA metabolism.<sup>28</sup> We noted gene silencing by microRNA (miRNA) in particular. MiRNAs play a major role in mRNA metabolism. Psychiatric disorders such as schizophrenia and bipolar disorder have been linked to miRNA dysregulation and dysfunction.<sup>29</sup>

*CNOT1* is a large scaffolding subunit in the CCR4-NOT complex.<sup>30</sup> *CNOT1* plays an important role in the enzymatic activity of the CCR4-NOT complex and is critical to the control of mRNA deadenylation and mRNA exonucleolytic decay. Degradation of mRNA is initiated by the shortening of the poly (A) tail by the CCR4-NOT deadenylase complex. MiRNAs bind to miRNA-induced silencing

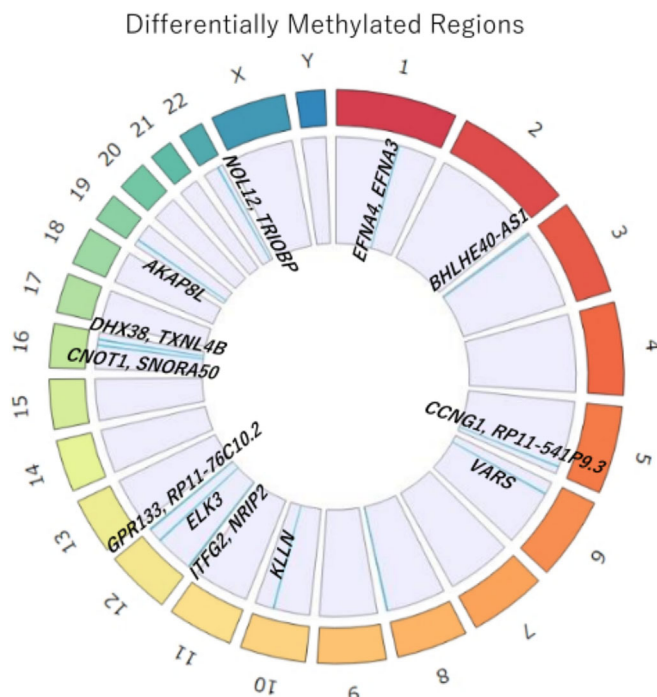


**FIGURE 2** The circos plot displaying the relative positioning of 13 DMRs on the chromosomes. This plot was created by the R package BioCircos. Numbers (1–22) and alphabets (X and Y) outside the circle indicate chromosome numbers. Chromosome coordinates increase along the clockwise direction. Blue bars indicate the relative positions of the DMRs on the chromosomes, and the genes contained in each DMR are pointed out. DMR: differentially methylated region

complexes to repress the translation of their target mRNAs and promote mRNA decay. *CNOT1* was shown to be involved in gene silencing by miRNAs through interactions with DEAD Box Protein 6.<sup>31</sup> The hypomethylation in the *CNOT1* gene observed in the current study suggests that the alterations in mRNA metabolism in patients with METH dependence may be similar to those suggested in schizophrenia and bipolar disorder, resulting in common symptoms such as psychosis.

*PUM1* showed overlap with significantly hypomethylated positions in the current study ( $q = 2.83 \times 10^{-2}$ ,  $p = 1.09 \times 10^{-7}$ ). This gene codes for PUmilio1 (PUM1), which also participates in mRNA metabolism.<sup>32</sup> Further, in the current GO analysis, several terms for mRNA metabolism exhibited  $p$  values  $<0.01$ . These terms included *CNOT1*, *PUM1*, and *EIF4ENIF1*.

## 4.2 | Relevance to several neurological disorders

Many previous studies have demonstrated that METH dependence causes neuropathy and substantia nigra deficits, which are also observed in Parkinson's disease.<sup>7,33</sup> Memory impairment and changes in hippocampal volume induced by METH administration are reminiscent of Alzheimer's disease.<sup>34,35</sup> The results of the current KEGG pathway analysis included pathways relevant to several neurological

disorders, including Parkinson's disease, prion disease, Huntington's disease, and Alzheimer's disease. These pathways included *TUBA8*, *PSMA6*, *MAPK8*, *NDUFS3*, and *NDUFS6*. DNA methylation at site cg21638645 ( $p = 4.25 \times 10^{-6}$  in this study), a probe associated with the *NDUFS6* gene, has been shown to correlate with prenatal exposure to perfluorononanoic acid (PFNA) in a previous study by Environ et al. Prenatal exposure to perfluoroalkyl substances (PFAS) and their congeners, including PFNA, have neuropsychiatric effects such as cognitive decline and late onset of puberty.<sup>36</sup>

In this GO analysis, the GO term for respirasomes showed relative enrichment. This term included *NDUFS3*, *NDUFS6*, and *TTC19*. Respirasome is a large molecular device that performs cellular respiration.<sup>37</sup> Mitochondrial respiratory chain supercomplexes (RCS) have been suggested to facilitate electron transport, reduce the production of reactive oxygen species (ROS), and maintain the structural integrity of individual electron transport chain complexes. Respirasome is a representative of the RCS. Disassembly of the RCS has been observed in neurodegenerative diseases, aging, cardiovascular diseases, and diabetes.<sup>38</sup> The levels of mitochondrial respiratory protein complexes I–V are reduced in the brain mitochondria in Parkinson's disease, implying a generalized defect in respirasome assembly.<sup>39</sup> Many neurodegenerative diseases (e.g., stroke) are caused by oxidative stress induced by impaired mitochondrial function and increased ROS or reactive nitrogen species.<sup>40</sup>

These results suggest that METH dependence causes changes in epigenetics mechanisms that could potentially provide neurological dysfunctions, corroborating the results of previous studies.

## 4.3 | Excitatory extracellular ligand-gated ion channel activity

The GO terms of excitatory extracellular ligand-gated ion channel activity were relatively enriched. These terms included *CHRNA2*, *GRIK2*, and *P2RX5*. A representative excitatory neurotransmitter in the brain is glutamate. There are three families of ionotropic receptors with intrinsic cation permeable channels. These are N-methyl-D-aspartate (NMDA), alpha-amino-3-hydroxy-5-methyl-4-isoxazolepropionic acid (AMPA), and kainate receptors.<sup>41–43</sup> Glutamatergic system is a potential therapeutic target for amnesia, anxiety, hyperalgesia, and psychosis, including schizophrenia.<sup>44–47</sup> The symptoms of these diseases have several common features with METH dependence; therefore, similar mechanisms may be caused by DNA methylation in METH dependence. Among genes of these terms, *GRIK2* ( $p = 2.43 \times 10^{-6}$ ), has been identified as a risk gene for obsessive-compulsive disorder.<sup>48</sup> This gene may be also associated with compulsive drug-seeking and intake behaviour in patients with METH dependence.

## 4.4 | BDNF-AS1

In the current study, the *BDNF-AS1* gene overlapped a DMP ( $p = 5.76 \times 10^{-6}$ ). While *BDNF* plays an important role in the survival



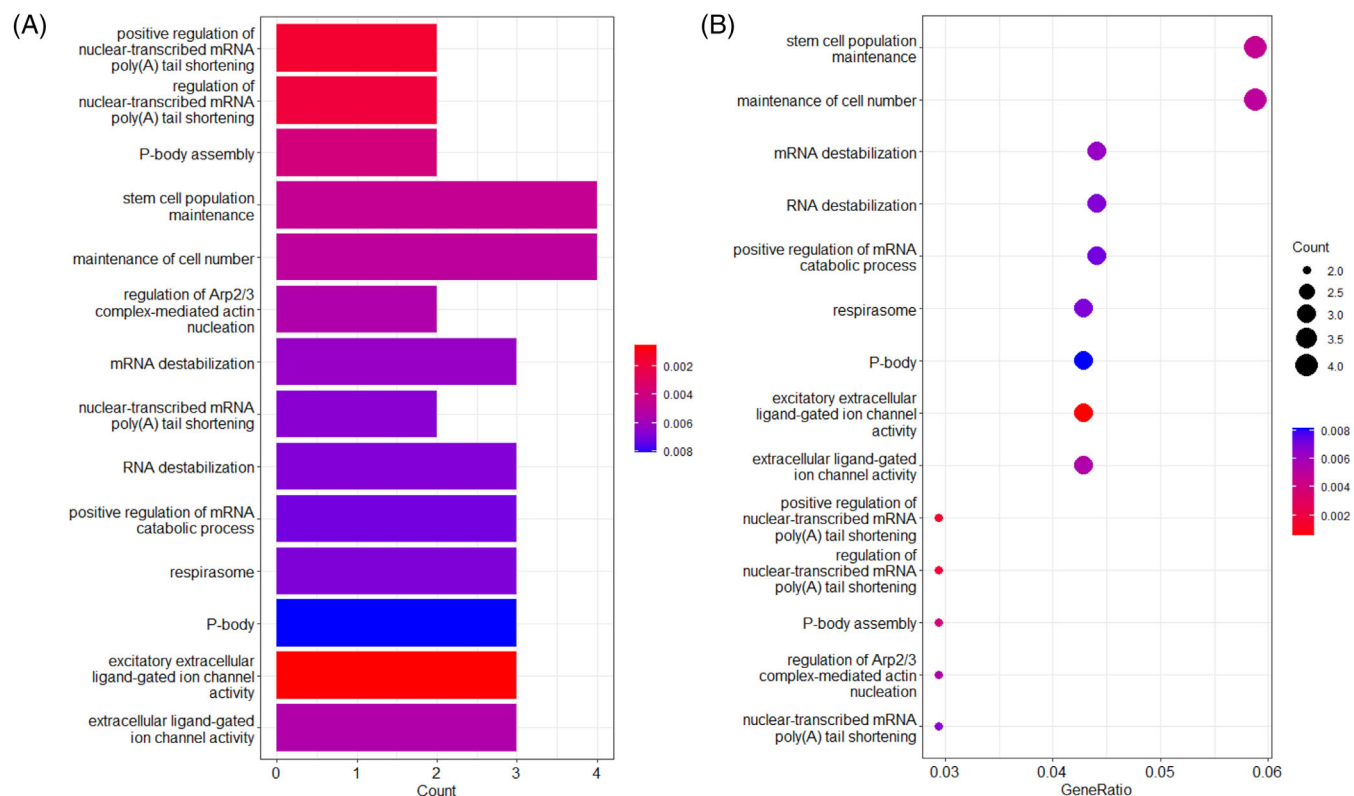


**FIGURE 3** (A) Bar plot of the terms that met the criterion of unadjusted  $p < 0.01$  in the GO analysis. The horizontal axis represents the number of overlapping genes in each term, and the colour of the bar varies according to the  $p$  value. The bar plots were created using the R package, clusterProfiler. (B) The dot plot of the terms with unadjusted  $p < 0.01$  in the GO analysis. The data were further sorted by the gene ratio. The horizontal axis indicates the ratio of overlapping genes in each term, the size of the circle varies according to the number of overlapping genes in each term, and the colour of the circle changes according to the  $p$  value. The dot plot was created using R package, clusterProfiler. GO: Gene Ontology

and differentiation of neurons, *BDNF-AS1* is known to repress the expression of the *BDNF* sense transcript.<sup>49,50</sup> Considering the various psychiatric symptoms in patients with METH dependence, it would be logical to assume that hypomethylation and overexpression of *BDNF-AS1* would decrease *BDNF* expression, leading to worsening of neuronal function. However, some other studies reported that *BDNF* levels were elevated in the hippocampus of rats that self-administered METH and in the plasma of human METH users.<sup>51,52</sup> Xu et al. utilized bisulfite pyrosequencing to reveal DNA hypomethylation at a position relevant to *BDNF*.<sup>22</sup> Some studies have suggested a positive correlation between *BDNF-AS* and *BDNF* expression.<sup>53,54</sup> Thus, we hypothesized that there may be a complex feedback mechanism, including an antisense mechanism and DNA methylation, between the two genes. Further, the relationship between changes in DNA methylation and changes in gene expression is proving to be more complex than previously thought.<sup>55</sup> *BDNF* is also associated with various psychiatric and neurological disorders, not only METH dependence.<sup>56,57</sup> At the very least, the current study suggests that the association between symptoms in patients with METH dependence, *BDNF* and *BDNF-AS1* cannot be ignored, similar to previous studies.

## 4.5 | Limitation

The current study has several limitations. We focused solely on DNA methylation in the blood samples and did not examine mRNA or protein expression, nor did we use other samples such as brain tissue. The relationship between changes in DNA methylation and in gene expression is more complex than previously thought.<sup>55</sup> Few genes showed significant DNA methylation changes, necessitating future studies with a larger sample size. Moreover, we did not use strict conditions in the enrichment analyses. All samples analysed in this study were obtained from individuals of Japanese descent. The frequency of patients with a history of smoking was significantly higher in the disease group. Because smoking affects DNA methylation, a history of smoking was included as a confounding factor in the analysis; however, it may not fully account for the close interaction between smoking and METH use.<sup>58</sup> We could not obtain information on other confounding factors such as education, adverse childhood experiences, physical activity, diet, and medication use. Cell type proportion was not included as a confounding factor for the main model, as there was no significant difference in each cell type between the two groups (Figure S1) and the sample size was small. Larger sample sizes

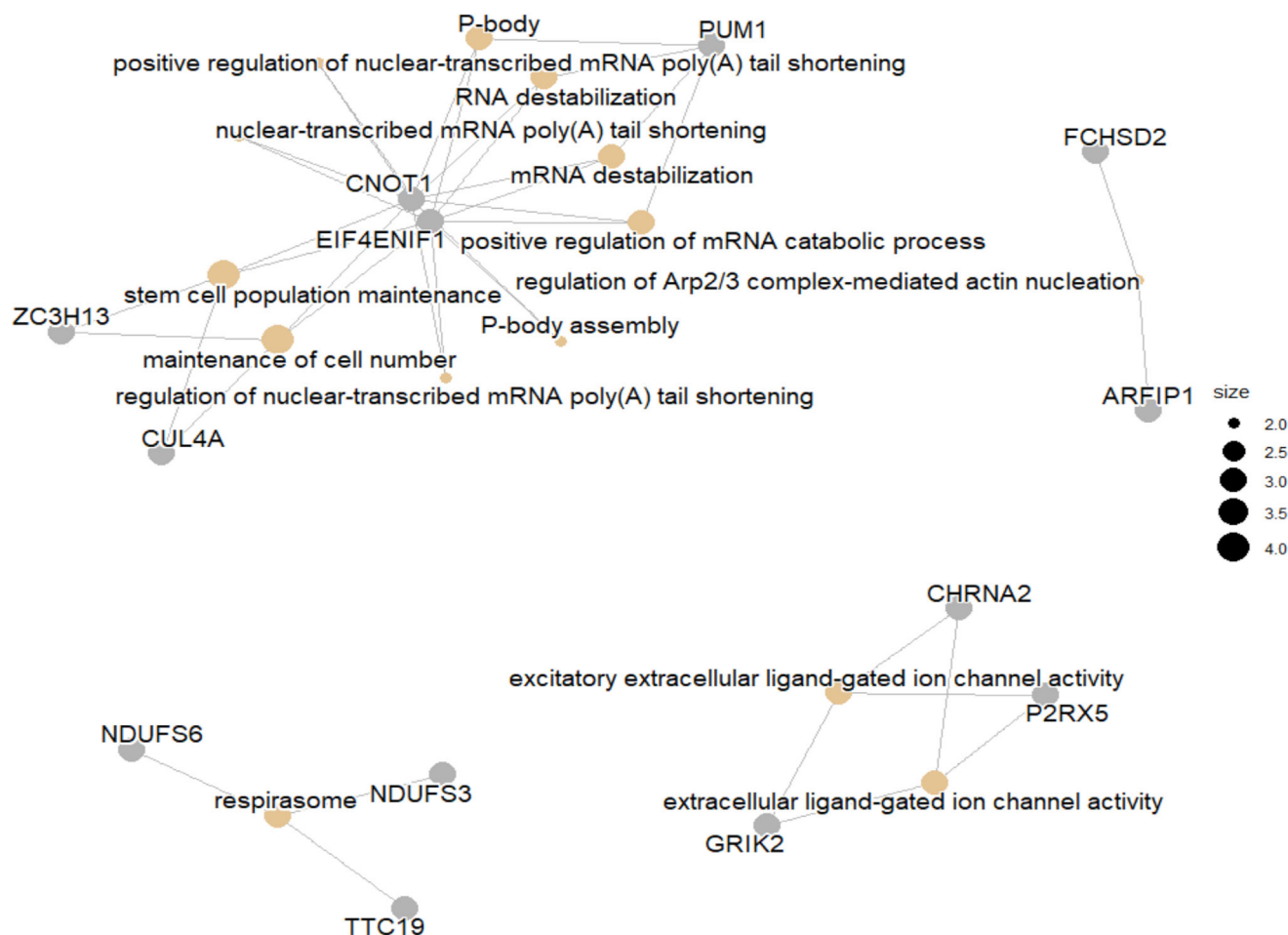


**FIGURE 4** Cnetplot of GO terms that met unadjusted  $p < 0.01$  and relevant genes. The cnetplot was created using the R package, clusterProfiler. The size of the orange sphere is determined by  $-\log_{10}(\text{unadjusted } p)$  for each term. GO: Gene Ontology

may further reveal DMPs, DMRs, and modules suggesting co-methylation that show significant associations with METH dependence. Despite the above-mentioned limitations, the results helped corroborate the findings of previous studies and revealed the relevance of genes that have rarely been mentioned in association with METH use. We hope that these findings will expand the range of genes that will be the focal points of future research and analysis.

## 5 | CONCLUSION

In the current EWAS, we examined the association between DNA methylation and METH dependence. METH dependence induces symptoms such as hallucinations, delusions, compulsive drug-seeking behaviour, compulsive drug-taking behaviour, and neurological symptoms, which share commonalities with a variety of other psychiatric disorders or neurodegenerative diseases. We identified several candidate genes (especially *CNOT1* and *PUM1*) and processes that may be responsible for these symptoms. We consider the possibility that these genes and processes are involved in the development of METH dependence symptoms. These warrant further investigation.

## AUTHOR CONTRIBUTIONS

**Toshiyuki Shirai:** Data curation; formal analysis; investigation; visualization; writing—original draft. **Satoshi Okazaki:** Conceptualization; data curation; supervision; writing—review and editing. **Takaki Tanifuji:** Data curation; resources. **Ikuo Otsuka:** Resources. **Tadasu Horai:** Resources. **Kentaro Mouri:** Resources. **Yukihiro Takemura:** Resources. **Katsuro Aso:** Resources. **Noriya Yamamoto:** Resources. **Akitoyo Hishimoto:** Conceptualization; supervision; writing—review and editing.

## ACKNOWLEDGEMENTS

We thank Yasuko Nagashima for technical assistance. This work was partially supported by the JSPS KAKENHI; grant numbers JP18K15483, JP21K07520 (S.O.) and JP17H04249 and JP21H02852 (A.H.).

## CONFLICT OF INTEREST STATEMENT

There are no conflicts of interest.

## DATA AVAILABILITY STATEMENT

The datasets of this study are available from the corresponding author upon reasonable request.

## ETHICS STATEMENT

The study was approved by the Ethics Committee of Genetics, Graduate School of Medicine, Kobe University. Written informed consent was obtained from all participants before the commencement of this study, in accordance with the Declaration of Helsinki.

## ORCID

Satoshi Okazaki  <https://orcid.org/0000-0001-5953-5526>

## REFERENCES

- Gold MS, Kobeissy FH, Wang KK, et al. Methamphetamine- and trauma-induced brain injuries: comparative cellular and molecular neurobiological substrates. *Biol Psychiatry*. 2009;66(2):118-127. doi:10.1016/j.biopsych.2009.02.021
- World Drug Report 2022. UNODC; 2022. Booklet 2.
- Jayanthi S, McCoy MT, Cadet JL. Epigenetic regulatory dynamics in models of methamphetamine-use disorder. *Genes (Basel)*. 2021;12(10):1614. doi:10.3390/genes12101614
- Cruickshank CC, Dyer KR. A review of the clinical pharmacology of methamphetamine. *Addiction*. 2009;104(7):1085-1099. doi:10.1111/j.1360-0443.2009.02564.x
- Bramness JG, Gundersen OH, Guterstam J, et al. Amphetamine-induced psychosis—a separate diagnostic entity or primary psychosis triggered in the vulnerable? *BMC Psychiatry*. 2012;12(1):221. doi:10.1186/1471-244X-12-221
- Cadet JL, Brannock C, Jayanthi S, Krasnova IN. Transcriptional and epigenetic substrates of methamphetamine addiction and withdrawal: evidence from a long-access self-administration model in the rat. *Mol Neurobiol*. 2015;51(2):696-717. doi:10.1007/s12035-014-8776-8
- Shin EJ, Jeong JH, Hwang Y, et al. Methamphetamine-induced dopaminergic neurotoxicity as a model of Parkinson's disease. *Arch Pharm Res*. 2021;44(7):668-688. doi:10.1007/s12272-021-01341-7
- Vause T, Jaksic H, Neil N, Frijters JC, Jackiewicz G, Feldman M. Functional behavior-based cognitive-behavioral therapy for obsessive compulsive behavior in children with autism spectrum disorder: a randomized controlled trial. *J Autism Dev Disord*. 2020;50(7):2375-2388. doi:10.1007/s10803-018-3772-x
- Wearne TA, Cornish JL. A comparison of methamphetamine-induced psychosis and schizophrenia: a review of positive, negative, and cognitive symptomatology. *Front Psych*. 2018;9:491. doi:10.3389/fpsy.2018.00491
- Yui K, Ikemoto S, Ishiguro T, Goto K. Studies of amphetamine or methamphetamine psychosis in Japan: relation of methamphetamine psychosis to schizophrenia. *Ann N Y Acad Sci*. 2000;914(1):1-12. doi:10.1111/j.1749-6632.2000.tb05178.x
- Cadet JL, Bisagno V, Milroy CM. Neuropathology of substance use disorders. *Acta Neuropathol*. 2014;127(1):91-107. doi:10.1007/s00401-013-1221-7
- Cadet JL, Krasnova IN, Jayanthi S, Lyles J. Neurotoxicity of substituted amphetamines: molecular and cellular mechanisms. *Neurotox Res*. 2007;11(3-4):183-202. doi:10.1007/BF03033567
- Rizzardi LF, Hickey PF, Rodriguez DiBlasi V, et al. Neuronal brain-region-specific DNA methylation and chromatin accessibility are associated with neuropsychiatric trait heritability. *Nat Neurosci*. 2019;22(2):307-316. doi:10.1038/s41593-018-0297-8
- Rodriguez RM, Suarez-Alvarez B, Mosén-Ansorena D, et al. Regulation of the transcriptional program by DNA methylation during human  $\alpha\beta$  T-cell development. *Nucleic Acids Res*. 2015;43(2):760-774. doi:10.1093/nar/gku1340
- Baylin SB. DNA methylation and gene silencing in cancer. *Nat Clin Pract Oncol*. 2005;2(Suppl 1):S4-S11. doi:10.1038/ncponc0354
- Razin A, Cedar H. DNA methylation and gene expression. *Microbiol Rev*. 1991;55(3):451-458. doi:10.1128/mr.55.3.451-458.1991
- Bird A. Perceptions of epigenetics. *Nature*. 2007;447(7143):396-398. doi:10.1038/nature05913
- Ho PJ, Dorajoo R, Ivanković I, et al. DNA methylation and breast cancer-associated variants. *Breast Cancer Res Treat*. 2021;188(3):713-727. doi:10.1007/s10549-021-06185-9
- Vaillancourt K, Yang J, Chen GG, et al. Cocaine-related DNA methylation in caudate neurons alters 3D chromatin structure of the IRXA gene cluster. *Mol Psychiatry*. 2021;26(7):3134-3151. doi:10.1038/s41380-020-00909-x
- Hao L, Luo T, Dong H, Tang A, Hao W. CHN2 promoter methylation change may be associated with methamphetamine dependence. *Shanghai Arch Psychiatry*. 2017;29(6):357-364. doi:10.11919/j.issn.1002-0829.217100
- Liu L, Luo T, Dong H, et al. Genome-wide DNA methylation analysis in male methamphetamine users with different addiction qualities. *Front Psych*. 2020;11:588229. doi:10.3389/fpsy.2020.588229
- Xu X, Ji H, Liu G, et al. A significant association between BDNF promoter methylation and the risk of drug addiction. *Gene*. 2016;584(1):54-59. doi:10.1016/j.gene.2016.03.010
- Godino A, Jayanthi S, Cadet JL. Epigenetic landscape of amphetamine and methamphetamine addiction in rodents. *Epigenetics*. 2015;10(7):574-580. doi:10.1080/15592294.2015.1055441
- Takemura Y, Tanifuji T, Okazaki S, et al. Epigenetic clock analysis in methamphetamine dependence. *Psychiatry Res*. 2022;317:114901. doi:10.1016/j.psychres.2022.114901
- Horvath S. DNA methylation age of human tissues and cell types. *Genome Biol*. 2013;14(10):R115. doi:10.1186/gb-2013-14-10-r115
- Houseman EA, Accomando WP, Koestler DC, et al. DNA methylation arrays as surrogate measures of cell mixture distribution. *BMC Bioinformatics*. 2012;13(1):86. doi:10.1186/1471-2105-13-86
- Peters TJ, Buckley MJ, Satham AL, et al. De novo identification of differentially methylated regions in the human genome. *Epigenetics Chromatin*. 2015;8(1):6. doi:10.1186/1756-8935-8-6
- Ito K, Takahashi A, Morita M, Suzuki T, Yamamoto T. The role of the CNOT1 subunit of the CCR4-NOT complex in mRNA deadenylation and cell viability. *Protein Cell*. 2011;2(9):755-763. doi:10.1007/s13238-011-1092-4
- Geaghan M, Cairns MJ. MicroRNA and posttranscriptional dysregulation in psychiatry. *Biol Psychiatry*. 2015;78(4):231-239. doi:10.1016/j.biopsych.2014.12.009
- Vissers L, Kalvakuri S, de Boer E, et al. De novo variants in CNOT1, a central component of the CCR4-NOT complex involved in gene expression and RNA and protein stability, cause neurodevelopmental delay. *Am J Hum Genet*. 2020;107(1):164-172. doi:10.1016/j.ajhg.2020.05.017
- Rouya C, Siddiqui N, Morita M, Duchaine TF, Fabian MR, Sonenberg N. Human DDX6 effects miRNA-mediated gene silencing via direct binding to CNOT1. *RNA*. 2014;20(9):1398-1409. doi:10.1261/ma.045302.114
- Zhou Y, Ng DY, Richards AM, Wang P. Loss of full-length pumilio 1 abrogates miRNA-221-induced gene p27 silencing-mediated cell proliferation in the heart. *Mol Ther Nucleic Acids*. 2022;27:456-470. doi:10.1016/j.omtn.2021.12.012
- Graves SM, Schwarzschild SE, Tai RA, Chen Y, Surmeier DJ. Mitochondrial oxidant stress mediates methamphetamine neurotoxicity in substantia nigra dopaminergic neurons. *Neurobiol Dis*. 2021;156:105409. doi:10.1016/j.nbd.2021.105409
- Golsorkhdan SA, Boroujeni ME, Aliaghaj A, et al. Methamphetamine administration impairs behavior, memory and underlying signaling pathways in the hippocampus. *Behav Brain Res*. 2020;379:112300. doi:10.1016/j.bbr.2019.112300

35. Ru Q, Tian X, Xiong Q, Xu C, Chen L, Wu Y. Krill oil alleviated methamphetamine-induced memory impairment via the MAPK signaling pathway and dopaminergic synapse pathway. *Front Pharmacol*. 2021;12:756822. doi:[10.3389/fphar.2021.756822](https://doi.org/10.3389/fphar.2021.756822)
36. Liu Y, Eliot MN, Papandonatos GD, et al. Gestational perfluoroalkyl substance exposure and DNA methylation at birth and 12 years of age: a longitudinal epigenome-wide association study. *Environ Health Perspect*. 2022;130(3):37005. doi:[10.1289/EHP10118](https://doi.org/10.1289/EHP10118)
37. Guo R, Gu J, Wu M, Yang M. Amazing structure of respirasome: unveiling the secrets of cell respiration. *Protein Cell*. 2016;7(12):854-865. doi:[10.1007/s13238-016-0329-7](https://doi.org/10.1007/s13238-016-0329-7)
38. Chapa-Dubocq XR, Rodríguez-Graciani KM, Guzmán-Hernández RA, Jang S, Brookes PS, Javadov S. Cardiac function is not susceptible to moderate disassembly of mitochondrial respiratory supercomplexes. *Int J Mol Sci*. 2020;21(5):1555. doi:[10.3390/ijms21051555](https://doi.org/10.3390/ijms21051555)
39. Arthur CR, Morton SL, Dunham LD, Keeney PM, Bennett JP Jr. Parkinson's disease brain mitochondria have impaired respirasome assembly, age-related increases in distribution of oxidative damage to mtDNA and no differences in heteroplasmic mtDNA mutation abundance. *Mol Neurodegener*. 2009;4(37):37. doi:[10.1186/1750-1326-4-37](https://doi.org/10.1186/1750-1326-4-37)
40. Anwar MR, Saldana-Caboverde A, Garcia S, Diaz F. The organization of mitochondrial supercomplexes is modulated by oxidative stress in vivo in mouse models of mitochondrial encephalopathy. *Int J Mol Sci*. 2018;19(6):1582. doi:[10.3390/ijms19061582](https://doi.org/10.3390/ijms19061582)
41. Meldrum BS. Glutamate as a neurotransmitter in the brain: review of physiology and pathology. *J Nutr*. 2000;130(4S Suppl):1007s-1015s. doi:[10.1093/jn/130.4.1007S](https://doi.org/10.1093/jn/130.4.1007S)
42. Tokarska A, Silberberg G. GABAergic interneurons expressing the  $\alpha 2$  nicotinic receptor subunit are functionally integrated in the striatal microcircuit. *Cell Rep*. 2022;39(8):110842. doi:[10.1016/j.celrep.2022.110842](https://doi.org/10.1016/j.celrep.2022.110842)
43. Lanore F, Labrousse VF, Szabo Z, Normand E, Blanchet C, Mulle C. Deficits in morphofunctional maturation of hippocampal mossy fiber synapses in a mouse model of intellectual disability. *J Neurosci*. 2012;32(49):17882-17893. doi:[10.1523/JNEUROSCI.2049-12.2012](https://doi.org/10.1523/JNEUROSCI.2049-12.2012)
44. Goff DC, Wine L. Glutamate in schizophrenia: clinical and research implications. *Schizophr Res*. 1997;27(2-3):157-168. doi:[10.1016/S0920-9964\(97\)00079-0](https://doi.org/10.1016/S0920-9964(97)00079-0)
45. Bennett AD, Everhart AW, Hulsebosch CE. Intrathecal administration of an NMDA or a non-NMDA receptor antagonist reduces mechanical but not thermal allodynia in a rodent model of chronic central pain after spinal cord injury. *Brain Res*. 2000;859(1):72-82. doi:[10.1016/S0006-8993\(99\)02483-X](https://doi.org/10.1016/S0006-8993(99)02483-X)
46. Helton DR, Tizzano JP, Monn JA, Schoepp DD, Kallman MJ. Anxiolytic and side-effect profile of LY354740: a potent, highly selective, orally active agonist for group II metabotropic glutamate receptors. *J Pharmacol Exp Ther*. 1998;284(2):651-660.
47. Lynch G, Granger R, Ambros-Ingerson J, Davis CM, Kessler M, Schehr R. Evidence that a positive modulator of AMPA-type glutamate receptors improves delayed recall in aged humans. *Exp Neurol*. 1997;145(1):89-92. doi:[10.1006/exnr.1997.6447](https://doi.org/10.1006/exnr.1997.6447)
48. Arnold PD, Kathleen D, Askland CB, Bellodi L, et al. Revealing the complex genetic architecture of obsessive-compulsive disorder using meta-analysis. *Mol Psychiatry*. 2018;23(5):1181-1188. doi:[10.1038/mp.2017.154](https://doi.org/10.1038/mp.2017.154)
49. Chiou YJ, Huang TL. Brain-derived neurotrophic factor (BDNF) and bipolar disorder. *Psychiatry Res*. 2019;274:395-399. doi:[10.1016/j.psychres.2019.02.051](https://doi.org/10.1016/j.psychres.2019.02.051)
50. Jun R, Zhang W, Beacher NJ, Zhang Y, Li Y, Lin DT. Dysbindin-1, BDNF, and GABAergic transmission in schizophrenia. *Front Psych*. 2022;13:876749. doi:[10.3389/fpsy.2022.876749](https://doi.org/10.3389/fpsy.2022.876749)
51. Kim DJ, Roh S, Kim Y, et al. High concentrations of plasma brain-derived neurotrophic factor in methamphetamine users. *Neurosci Lett*. 2005;388(2):112-115. doi:[10.1016/j.neulet.2005.06.042](https://doi.org/10.1016/j.neulet.2005.06.042)
52. McFadden LM, Vieira-Brock PL, Hanson GR, Fleckenstein AE. Methamphetamine self-administration attenuates hippocampal serotonergic deficits: role of brain-derived neurotrophic factor. *Int J Neuropsychopharmacol*. 2014;17(8):1315-1320. doi:[10.1017/S1461145714000327](https://doi.org/10.1017/S1461145714000327)
53. Esfandi F, Bouraghi H, Glassy MC, et al. Brain-derived neurotrophic factor downregulation in gastric cancer. *J Cell Biochem*. 2019;120(10):17831-17837. doi:[10.1002/jcb.29050](https://doi.org/10.1002/jcb.29050)
54. Ghafouri-Fard S, Khoshbakht T, Taheri M, Ghanbari M. A concise review on the role of BDNF-AS in human disorders. *Biomed Pharmacother*. 2021;142:112051. doi:[10.1016/j.biopha.2021.112051](https://doi.org/10.1016/j.biopha.2021.112051)
55. van Eijk KR, de Jong S, Boks MP, et al. Genetic analysis of DNA methylation and gene expression levels in whole blood of healthy human subjects. *BMC Genomics*. 2012;13(1):636. doi:[10.1186/1471-2164-13-636](https://doi.org/10.1186/1471-2164-13-636)
56. Auta J, Smith RC, Dong E, et al. DNA-methylation gene network dysregulation in peripheral blood lymphocytes of schizophrenia patients. *Schizophr Res*. 2013;150(1):312-318. doi:[10.1016/j.schres.2013.07.030](https://doi.org/10.1016/j.schres.2013.07.030)
57. Chang L, Wang Y, Ji H, et al. Elevation of peripheral BDNF promoter methylation links to the risk of Alzheimer's disease. *PLoS ONE*. 2014;9(11):e110773. doi:[10.1371/journal.pone.0110773](https://doi.org/10.1371/journal.pone.0110773)
58. Zhang Y, Wilson R, Heiss J, et al. DNA methylation signatures in peripheral blood strongly predict all-cause mortality. *Nat Commun*. 2017;8(1):14617. doi:[10.1038/ncomms14617](https://doi.org/10.1038/ncomms14617)

## SUPPORTING INFORMATION

Additional supporting information can be found online in the Supporting Information section at the end of this article.

**How to cite this article:** Shirai T, Okazaki S, Tanifuji T, et al. Epigenome-wide association study on methamphetamine dependence. *Addiction Biology*. 2024;29(3):e13383. doi:[10.1111/adb.13383](https://doi.org/10.1111/adb.13383)